Amplitude, Competition, Self-Locking, Beat Frequency, and Time Development in a Three-Mode Gas Laser

M. D. Sayers* and L. Allen
School of Mathematical and Physical Sciences, University of Sussex, Falmer, Brighton, England
(Received 2 February 1970)

The unabbreviated Lamb semiclassical equations for the case of three interacting modes are numerically solved for a variety of laser parameters. Steady-state solutions are obtained for the amplitudes, beat frequencies, and time development of the modes by using the Kutta-Merson method of integration. It is found that for some solutions the relative phase angle ψ becomes constant, and so it is clear under what conditions self-locking is possible. When the modes are unlocked, the value of ψ varies with time even after the steady-state amplitudes have been achieved. Comparison is made with the locking criteria predicted by approaches to the theory where approximations have been made. A physical interpretation is given for the presence or absence of self-locking in terms of competition and of the ratio $\Delta/\Delta\nu_D$. Some general rules are established for the behavior of the rise time and delay of the onset of oscillation of the three modes.

I. INTRODUCTION

The Lamb[1] semiclassical theory of the laser enabled a discussion of threshold conditions, output as a function of cavity tuning, frequency pulling and pushing, mode competition, locking, population pulsations, and related phenomena to be discussed within a single framework. Prior to this paper, development of laser theory had been fragmentary. Schawlow and Townes[2] had discussed threshold conditions and Bennett[3] mode pulling and pushing, but a rigorous multimode theory had not been devised. Investigation of mode behavior via the study of beat notes between modes in gas lasers was carried out by Javan[4] and the beat frequencies found confirmed the existence of axial and transverse modes as predicted by Fox and Li.[5] After the Lamb theory was published, Fork and Pollack[6] computed the mode intensities and beat frequencies for the case of two axial modes as a function of resonator tuning but not for the case of variable population inversion $\overline{N}$ or of cavity Q. McFarlane[7] compared measurements of the beat frequency between two axial modes of a laser as a function of detuning with those predicted by the Lamb theory, but the mode interaction terms were dropped in his analysis. More recently, Allen, Jones, and Sayers[8] have investigated the variation with cavity Q of the beat frequency between axial modes of a gas laser taking into account all the interaction terms which exist in Lamb's formulation for three modes. The method of approach used was to solve the steady-state equations making use of the assumption that terms of the form $\eta_{ij}\sin\psi - \xi_{ij}\cos\psi$ in Lamb's equation (108) have a time average of zero, since the "relative phase angle" between the three modes ψ is itself rapidly increasing with time. This implies that no locking takes place. Within the framework of these assumptions, the beat frequencies predicted for three modes in the He-Ne 0.633-μm and 1.15-μm laser transitions were confirmed experimentally.

The phenomenon of mode locking was apparently first seen by Javan in 1964. Crowell[9] observed self-locking in a He-Ne 0.633-μm laser, and Gaddy and Schaefer[10] observed similar effects in an Ar^+ laser operating at 0.488 μm. Uchida[11] gave a very useful exposition of mode interactions in gas lasers using the Lamb formulation. The problem of self-locking was considered by introducing an external source term which may, in fact, be internally generated by noise or may be a combination tone. In a following paper with Ueki,[12] Uchida presented an experimental and theoretical examination of mode structure and locking phenomena, but ignored many of Lamb's interaction terms. Jones, Sayers, and Allen[13] derived approximate conditions under which self-locking can occur in a gas laser. The results suggested that self-locking should be a fairly common occurrence, and this was demonstrated to be the case with experiments performed on He-Ne 0.633-μm and 1.15-μm lasers. This analysis depended strongly upon the assumption that the mode amplitudes retain the values they would have in the absence of mode competition. However, some general, but oversimple rules of behavior for the occurrence of mode locking in three-mode gas lasers were derived and detailed beat frequency predictions verified with a He-Ne laser. The whole problem of mode locking in lasers is extensively reviewed by Allen and Jones.[14]

In this work, an attempt is made at a rigorous solution of Lamb's equations for the interesting problem of three-mode operation in the presence of mode interactions and competition in the completely general case. It is found by solving the

differential equations describing mode behavior rather than the steady-state equations, that mode amplitudes may be calculated and the relative phase angle computed so that it becomes immediately clear whether the modes are locked or unlocked. Mode amplitudes and the value of the relative phase ψ are investigated for the atomic parameters of real laser systems in order to make the calculations of specific interest, and for a range of detunings and cavity Q's. Use of the differential equations allows the time development of the modes to be discussed and some conclusions are drawn concerning the rate of growth of a laser mode in a three-mode environment. When the relative phase angle indicates that locking is taking place the same techniques allow the beat frequencies to be computed but this time, unlike our earlier work,[13] all mode interactions have been taken into account.

It should, of course, be realized that the intrinsic faults of the Lamb theory are equally the faults of the work presented here. The effect of spontaneous emission on the laser transition is not taken into account; the mode distributions are considered to have no spatial variation[15]; the fields are not allowed to grow from zero, because of the nature of the self-consistent approach used by Lamb; and the discussion takes place in the Doppler limit of $\Delta\nu_D \gg \gamma_{ab}, \Delta$. The Doppler gain curve is considered to be symmetric and hence the calculations are only valid for a single Ne isotope He-Ne laser.

II. THEORY

The three-mode amplitude determining equations given by Lamb[1] are

$$\begin{aligned}
\dot{E}_1 &= \alpha_1 E_1 - \beta_1 E_1^3 - \theta_{12} E_1 E_2^2 - \theta_{13} E_1 E_3^2 \\
&\quad - (\eta_{23}\cos\psi + \xi_{23}\sin\psi) E_2^2 E_3 \ , \\
\dot{E}_2 &= \alpha_2 E_2 - \beta_2 E_2^3 - \theta_{21} E_2 E_1^2 - \theta_{23} E_2 E_3^2 \\
&\quad - (\eta_{13}\cos\psi - \xi_{13}\sin\psi) E_1 E_2 E_3 \ , \\
\dot{E}_3 &= \alpha_3 E_3 - \beta_3 E_3^3 - \theta_{31} E_3 E_1^2 - \theta_{32} E_3 E_2^2 \\
&\quad - (\eta_{21}\cos\psi + \xi_{21}\sin\psi) E_2^2 E_1 \ ,
\end{aligned} \tag{1}$$

where the relative phase angle ψ is defined as

$$\psi = (2\nu_2 - \nu_1 - \nu_3)t + (2\phi_2 - \phi_1 - \phi_3) \ .$$

The influence of mode coupling can be seen by considering its effect on the equation for $\dot{E}_1$. In the absence of any interaction, the equation of motion for E_1 would be $\dot{E}_1 = \alpha_1 E_1 - \beta_1 E_1^3$ the familiar single-mode equation, where α_1 describes the gain and β_1 describes the saturation. The effect of the interaction terms which take into account E_2 and E_3 can be thought of as lowering the effective gain. α_1 is effectively replaced by $\alpha_1 - \theta_{12}E_2^2 - \theta_{13}E_3^2$. The remaining terms in $\cos\psi$ and $\sin\psi$ describe the phase-dependent coupling. If it is assumed that there is no locking, then ψ is a rapidly oscillating function of time, and hence the average values of $\sin\psi$ and $\cos\psi$ will be zero. Under these conditions, the set of equations (1) reverts to the unlocked three-mode equations as used by Allen, Jones, and Sayers.[8]

The frequency-determining equations given by Lamb are

$$\begin{aligned}
\nu_1 + \dot{\phi}_1 &= \Omega_1 + \sigma_1 + \rho_1 E_1^2 + \tau_{12} E_2^2 + \tau_{13} E_3^2 \\
&\quad - E_2^2 E_3 E_1^{-1}(\eta_{23}\sin\psi - \xi_{23}\cos\psi) \ , \\
\nu_2 + \dot{\phi}_2 &= \Omega_2 + \sigma_2 + \rho_2 E_2^2 + \tau_{21} E_1^2 + \tau_{23} E_3^2 \\
&\quad + E_1 E_3(\eta_{13}\sin\psi + \xi_{13}\cos\psi) \ , \\
\nu_3 + \dot{\phi}_3 &= \Omega_3 + \sigma_3 + \rho_3 E_3^2 + \tau_{31} E_1^2 + \tau_{32} E_2^2 \\
&\quad - E_2^2 E_1 E_3^{-1}(\eta_{21}\sin\psi - \xi_{21}\cos\psi) \ .
\end{aligned} \tag{2}$$

From these, an expression for $\dot{\psi}$ can be obtained:

$$\dot{\psi} = \Sigma + A\sin\psi + B\cos\psi \ , \tag{3}$$

where
$$\begin{aligned}
\Sigma &= 2\sigma_2 - \sigma_1 - \sigma_3 + E_1^2(2\tau_{21} - \rho_1 - \tau_{31}) \\
&\quad + E_2^2(2\rho_2 - \tau_{12} - \tau_{32}) + E_3^2(2\tau_{23} - \tau_{13} - \rho_3) \ , \\
A &= 2E_1 E_3\,\eta_{13} + E_2^2 E_3\, E_1^{-1}\eta_{23} + E_2^2 E_1\, E_3^{-1}\eta_{21} \ , \\
B &= 2E_1 E_3 \xi_{13} - E_2^2 E_3 E_1^{-1}\xi_{23} - E_2^2 E_1 E_3^{-1}\xi_{21} \ .
\end{aligned}$$

There are some misprints involving the signs[16] of the ψ terms in the amplitude- and frequency-determining equations in Lamb's paper, which have been corrected here.

Since $\psi = \Sigma + A\sin\psi + B\cos\psi$, it can be seen that

$$t(\psi) = \int_{\psi_0}^{\psi} \frac{d\psi}{\Sigma + A\sin\psi + B\cos\psi} \ .$$

The interesting case is when $\Sigma \leqslant (A^2 + B^2)^{1/2}$, for then the denominator can pass through zero giving a pole in the solution of the integral. This occurs when ψ reaches its asymptotic value

$$\psi = -\sin^{-1}\left(\frac{\Sigma}{(A^2 + B^2)^{1/2}}\right) \ .$$

Since there is then no linear dependence of ψ on t, it means that $2\nu_2 - \nu_1 - \nu_3 = 0$ and hence that $\nu_3 - \nu_2 = \nu_2 - \nu_1$, giving frequency locking with a definite phase angle $\psi = 2\phi_2 - \phi_1 - \phi_3$. Thus, $A^2 + B^2 \geqslant \Sigma^2$ gives a convenient criterion for the occurrence of locking. Whether or not the criterion is satisfied clearly depends on the detuning of the cavity modes from the line center, the depth of the "holes" burnt into the gain curve and hence the intensity, and the atomic parameters of the system such as the decay constants γ_a, γ_b and γ_{ab}, the axial mode spacing Δ, and the spatial Fourier components of the inversion density $\bar{N}$

and N_2. In Jones, Sayers, and Allen,[13] the criterion was simplified and evaluated for three modes in terms of these parameters.

All methods, however, which rely on values of the mode intensities which are calculated in some way from the unlocked equations, in order to estimate the size of $A^2+B^2-\Sigma^2$, can provide at best only a guide as to the probability of whether or not locking will occur. In order to gain any degree of rigor in the calculations it is necessary to solve the set of differential equations (1) for given initial conditions and given values of the atomic parameters and to see whether locking does, in fact, occur. The methods used in Allen, Jones, and Sayers[8] assumed that a steady state had been reached in which $\dot{E}_1=\dot{E}_2=\dot{E}_2=0$ and that the steady-state field amplitudes could be found by solving the steady-state equations. In order to determine the conditions under which locking can take place, it is necessary to allow ψ to be free either to become constant (locked situation) or to continue to increase with time (unlocked situation). It therefore becomes necessary to solve the set of equations (1) as a set of four first-order differential equations in the four variables E_1, E_2, E_3, ψ of the general form $\dot{\underline{y}}=f(\underline{y})$, where $f(y)$ is furnished from the equations for $\dot{E}_1$, $\dot{E}_2$, $\dot{E}_3$ from (1) and the equation for $\dot{\psi}$ from (3).

It is found that the solutions are not strongly dependent on the initial conditions. The mode amplitudes are found to grow rapidly if started from initial values 10^{-5} times less than their final steady-state values. In order to speed up the process of integration, in those calculations where detailed analysis of the full time development was not required, the unlocked steady-state values were used as initial conditions for the mode amplitudes.

The form of the parameters β, ρ, θ, τ, η, and ξ can be simplified for the purposes of computation by expressing all frequencies in units of the passive cavity mode spacing Δ. In this formalism, the detuning of the central mode from the line center can be written in terms of a dimensionless parameter a such that $\nu_n-\omega=a\Delta$. In this present work, a is used to describe the detuning of the central mode from the line center and the detunings of the remaining modes, and combination frequencies in the polarization are calculated accordingly.

The expressions for θ_{ij}, τ_{ij}, ρ_n, σ_n reduce simply to functions of a because the frequencies occur only as differences. In this new formalism, the parameters now become

$$\beta_1=A[1+\gamma_{ab}^2\,\mathfrak{L}((a-1)\Delta)],\quad \beta_2=A[1+\gamma_{ab}^2\,\mathfrak{L}(a\Delta)],\quad \beta_3=A[1+\gamma_{ab}^2\,\mathfrak{L}((a+1)\Delta)]\ ,$$

$$\rho_1=A\gamma_{ab}(a-1)\Delta\,\mathfrak{L}((a-1)\Delta),\quad \rho_2=A\gamma_{ab}a\Delta\,\mathfrak{L}(a\Delta),\quad \rho_3=A\gamma_{ab}(a+1)\Delta\,\mathfrak{L}((a+1)\Delta)\ ,$$

$$\theta_{12}=A\{\gamma_{ab}^2\,\mathfrak{L}((\tfrac{1}{2}-a)\Delta)+4\gamma_{ab}^2\Delta^{-2}-2\gamma_a\gamma_b\Delta^{-2}+(N_2/\bar{N})\gamma_a\gamma_b\mathfrak{L}((1-a)\Delta)[\gamma_{ab}^2-(1-a)\Delta^2]\Delta^{-2}\}\ ,$$

$$\theta_{21}=A\{\gamma_{ab}^2\,\mathfrak{L}((\tfrac{1}{2}-a)\Delta)+4\gamma_{ab}^2\Delta^{-2}-2\gamma_a\gamma_b\Delta^{-2}+(N_2/\bar{N})\gamma_a\gamma_b\,\mathfrak{L}(-a\Delta)[\gamma_{ab}^2-a\Delta^2]\Delta^{-2}\}\ ,$$

$$\theta_{13}=\theta_{31}=A\{\gamma_{ab}^2\,\mathfrak{L}(-a\Delta)+\gamma_{ab}^2\Delta^{-2}-\tfrac{1}{2}(\gamma_a\gamma_b)\Delta^{-2}\},$$

$$\theta_{23}=A\{\gamma_{ab}^2\,\mathfrak{L}((-\tfrac{1}{2}-a)\Delta)+4\gamma_{ab}^2\Delta^{-2}+(N_2/\bar{N})\gamma_a\gamma_b\,\mathfrak{L}(-a\Delta)(\gamma_{ab}^2+a\Delta^2)\Delta^{-2}-2\gamma_a\gamma_b\Delta^{-2}\},$$

$$\theta_{32}=A\{\gamma_{ab}^2\,\mathfrak{L}((-\tfrac{1}{2}-a)\Delta)+4\gamma_{ab}^2\Delta^{-2}+(N_2/\bar{N})\gamma_a\gamma_b\,\mathfrak{L}((-a-1)\Delta[\gamma_{ab}^2-(a-1)\Delta^2]\Delta^{-2}-2\gamma_a\gamma_b\Delta^{-2}\}\ ,$$

$$\tau_{12}=-A[\gamma_{ab}(\tfrac{1}{2}-a)\mathfrak{L}((\tfrac{1}{2}-a)\Delta)+2\gamma_{ab}\Delta^{-1}+(N_2/\bar{N})\gamma_a\gamma_b(2-a)\Delta\gamma_{ab}\mathfrak{L}((1-a)\Delta)\Delta^{-2}]\ ,$$

$$\tau_{21}=-A[\gamma_{ab}(\tfrac{1}{2}-a)\mathfrak{L}((\tfrac{1}{2}-a)\Delta)-2\gamma_{ab}\Delta^{-1}-(N_2/\bar{N})\gamma_a\gamma_b(1+a)\Delta\gamma_{ab}\,\mathfrak{L}(-a\Delta)\Delta^{-2}]\ ,$$

$$\tau_{13}=-A[\gamma_{ab}(-a\Delta)\mathfrak{L}(-a\Delta)+\gamma_{ab}\Delta^{-1}],\quad \tau_{31}=-A[\gamma_{ab}(-a\Delta)\mathfrak{L}(-a\Delta)-\gamma_{ab}\Delta^{-1}]\ ,$$

$$\tau_{23}=-A[\gamma_{ab}(-\tfrac{1}{2}-a)\Delta\,\mathfrak{L}((-\tfrac{1}{2}-a)\Delta)+2\gamma_{ab}\Delta^{-1}-(N_2/\bar{N})\gamma_a\gamma_b(a-1)\Delta\gamma_{ab}\mathfrak{L}(-a\Delta)\Delta^{-2}]\ ,$$

$$\tau_{32}=-A[\gamma_{ab}(-\tfrac{1}{2}-a)\Delta\,\mathfrak{L}((-\tfrac{1}{2}-a)\Delta)-2\gamma_{ab}\Delta^{-1}-(N_2/\bar{N})\gamma_a\gamma_b(a+2)\Delta\gamma_{ab}\,\mathfrak{L}(-(a+1)\Delta)\Delta^{-2}]\ ,$$

$$\xi_{21}=A\{(-\gamma_a\gamma_b/\Delta^2)(N_2/\bar{N})\gamma_{ab}(-a-\tfrac{3}{2})[\gamma_{ab}^2+(-a-\tfrac{1}{2})^2]^{-1}\}\ ,$$

$$\xi_{23}=A\{(-\gamma_a\gamma_b/\Delta^2)(N_2/\bar{N})\gamma_{ab}(\tfrac{3}{2}-a)[\gamma_{ab}^2+(\tfrac{1}{2}-a)^2]^{-1}\}\ ,$$

$$\xi_{13}=A\left[\frac{\gamma_a\gamma_b}{\Delta^2}\,\frac{N_2}{\bar{N}}\,\gamma_{ab}\left(\frac{(-a-\frac{3}{2})}{\gamma_{ab}^2+(-a-\frac{1}{2})^2}+\frac{(\frac{3}{2}-a)}{\gamma_{ab}^2+(\frac{1}{2}-a)^2}\right)\right]\ ,$$

$$\eta_{21}=A(\gamma_a\gamma_b/\Delta^2)\{(N_2/\bar{N})[\gamma_{ab}^2+(-a-\tfrac{1}{2})][\gamma_{ab}^2+(-a-\tfrac{1}{2})^2]^{-1}-1\}\ ,$$

$$\eta_{23}=A(\gamma_a\gamma_b/\Delta^2)\{(N_2/\bar{N})[\gamma_{ab}^2-(\tfrac{1}{2}-a)][\gamma_{ab}^2+(\tfrac{1}{2}-a)^2]^{-1}-1\}\ ,$$

$$\eta_{13}=A(\gamma_a\gamma_b/\Delta^2)\{(N_2/\bar{N})[\gamma_{ab}^2+(-a-\tfrac{1}{2})][\gamma_{ab}^2+(-a-\tfrac{1}{2})^2]^{-1}+(N_2/\bar{N})[\gamma_{ab}^2-(\tfrac{1}{2}-a)][\gamma_{ab}^2+(\tfrac{1}{2}-a)^2]^{-1}+2\},$$

where $A=\pi^{1/2}\nu\bar{N}\bar{\mu}^4/16\epsilon_0\hbar^3\gamma_a\gamma_b ku$.

Terms involving N_4 and higher orders of $N_{n-\mu}$ are neglected.

The constant A can be factored out from these interaction parameters, giving the advantage that N_2 does not appear explicitly but only as the ratio $N_2/\bar{N}$.

Lamb defines the spatial Fourier components of the inversion density as

$$N_{n-\mu}=(1/d)\int_0^d dz\,N(z)\cos(n-\mu)\,\pi z/d \ ,$$

where d is the length of the cavity. It is reasonable to assume a step-function distribution for $N(z)$ of the form

$$N(z)=0, \quad \text{for } z<z_0 \text{ and } z>z_0+l$$

$$N(z)=N, \quad \text{for } z_0\leq z\leq z_0+l \ ,$$

where l is the length of the plasma-tube discharge and z_0 is the distance of one end of the discharge from the nearest cavity mirror. $N_{(z)}$ is assumed to be uniform in the excited part of the tube.

Then $$\bar{N}=(N/d)\int_{z_0}^{z_0+l} dz=lN/d \ ,$$

$$N_2=\frac{1}{d}\int_{z_0}^{z_0+l} N\cos\frac{2\pi z}{d}\,dz$$

$$=\frac{N_2}{\pi}\cos\left(\frac{\pi(2z_0+l)}{d}\right)\sin\left(\frac{\pi l}{d}\right) \ .$$

The ratio $N_2/\bar{N}$ is

$$\frac{N_2}{\bar{N}}=\frac{d}{l\pi}\cos\left(\frac{\pi(2z_0+l)}{d}\right)\sin\left(\frac{\pi l}{d}\right),$$

which depends on the ratio of the active tube length to the cavity length and on the position of the tube with respect to the ends of the cavity.

With these considerations and using a series expansion for the plasma dispersion function $Z(\nu_n-\omega)$, all the parameters in Eq. (1) except α and σ can be calculated in terms of the atomic parameters.

The calculation of α presents a problem. It consists of two parts. One part represents the gain of the medium and the other the cavity losses. In order to evaluate α, the relative magnitude of these two parts must be determinable. The second part involves the excitation density $\bar{N}$ and this has been absorbed in the previous equations by the constant A. Fortunately it is possible to write this part in terms of the inserted loss L and the value of the inserted loss L_0 required to extinguish the laser, both of which are measurable.[17,18]

The expression for α_n obtained by this means[8] is

$$\alpha_n=\frac{\Delta}{2\pi}\left\{-\left(L+\frac{2\gamma_{ab}L_0}{ku\pi}\right)+L_0\exp\left[-\left(\frac{a-2+n}{ku}\right)\Delta\right]\right\},$$

where ku is 0.6 of the Doppler width. σ_n can be similarly evaluated to give

$$\sigma_n=\frac{\Delta}{2\pi}\,2L_0\left\{\left(\frac{a-2+n}{ku}\right)\Delta\,\frac{\gamma_{ab}}{ku}\exp\left[\left(\frac{\gamma_{ab}}{ku}\right)^2\right]\right.$$

$$\left.\times\exp\left[-\left(\frac{(a-2+n)}{ku}\,\Delta\right)^2\right]-2\left(\frac{a-2+n}{ku}\right)\Delta\right\}.$$

The constant A is still unevaluated and Eqs. (1) can be written in the form

$$\dot{E}_1=\alpha_1E_1-A[\beta_1'E_1^3-\phi_{12}'E_1E_2^2$$

$$+(\text{terms of order } E^3)] \ ,$$

and similarly for $\dot{E}_2$ and $\dot{E}_3$, where $\beta_1'=\beta/A$, etc.

Fortunately, the fact that all terms including A are of order E^3 can be exploited by making the substitution $E_n=A^{-1/2}E_n'$.

Then it can be shown that

$$\dot{E}_n'=\alpha_1E_1'-\beta_1'E_1'^3+\cdots, \quad \text{for } A^{-1/2}\neq 0 \ .$$

In the numerical solution of the equations, A was put equal to unity. The only effect of this is to introduce a scale factor of $A^{-1/2}$ in the value of the E_n's as the above discussion shows. In order to obtain absolute amplitudes, the values quoted in this paper should be multiplied by $A^{-1/2}$.

For each set of calculations, the values of the basic atomic parameters; $\Delta\nu_D$, the Doppler width; γ_a and γ_b, the upper and lower level decay parameters; γ_{ab}, the length of the cavity; the length of the tube; its disposition in the cavity; and the maximum inserted loss were chosen. The solution of the differential equations was then found as a function of inserted loss L and detuning a by a step-by-step numerical integration, using a Kutta-Merson method.[19] This work may be thought, in some sense, to be the self-locking equivalent of the work of McDuff and Harris who investigated FM- and AM-forced locking by numerical integration of the relevant equations.[20,21] In the present work, a grid of values of L and a was constructed and Eqs. (1) integrated at each point. Preliminary calculations were done for positive and negative detunings about the line center for one value of inserted loss only. These showed that the solutions were symmetric about the line center as they must be since the gain profile used was perfectly symmetric. This means that calculations only have to be done for

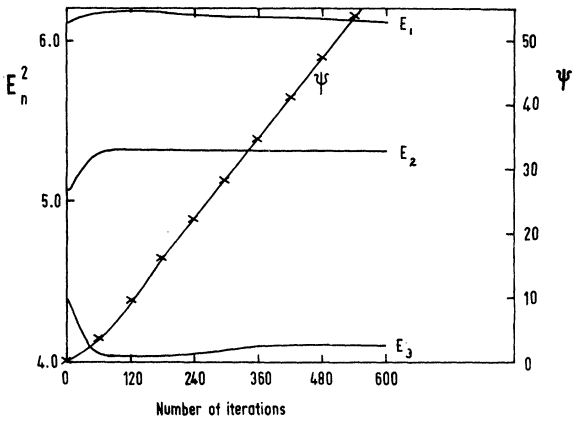

FIG. 1. Progress of the iterative solution to the equations for a typical set of parameters resulting in an unlocked steady state. The initial values of the E_n's are the steady-state solutions of the equations with terms involving ψ omitted.

detunings on one side of the line center, the results for the other side being determinable by symmetry. It was decided to use values of a of -0.4, -0.3, -0.2, -0.1, 0.0 (in units of the axial mode spacing Δ) and 10 values of inserted loss decreasing in uniform steps from the maximum inserted loss of 0.03. Two types of solution emerge from these calculations, one convergent and the other nonconvergent. In the convergent solution, the three mode amplitudes E_1, E_2, and E_3 and the relative phase angle ψ (which are the four dependent variables in the system) eventually become constant. This is the mode-locked situation. In the nonconvergent solution, the three mode amplitudes eventually become constant but the relative phase angle continues to increase with time. This is the unlocked steady state and it is found that the final values for E_1, E_2, and E_3 in this case are usually very close to those predicted by the unlocked theory except for the steady increase in ψ. Some cases, as the one shown in Fig. 1, show this behavior very clearly; but in others, particularly those away from the symmetric positions of detuning, the rounding errors in the computation accumulate and the values of the E_n's oscillate about the steady-state value and do not actually converge on it. In these cases, also, the relative phase angle continuously increases and they are therefore definitely to be

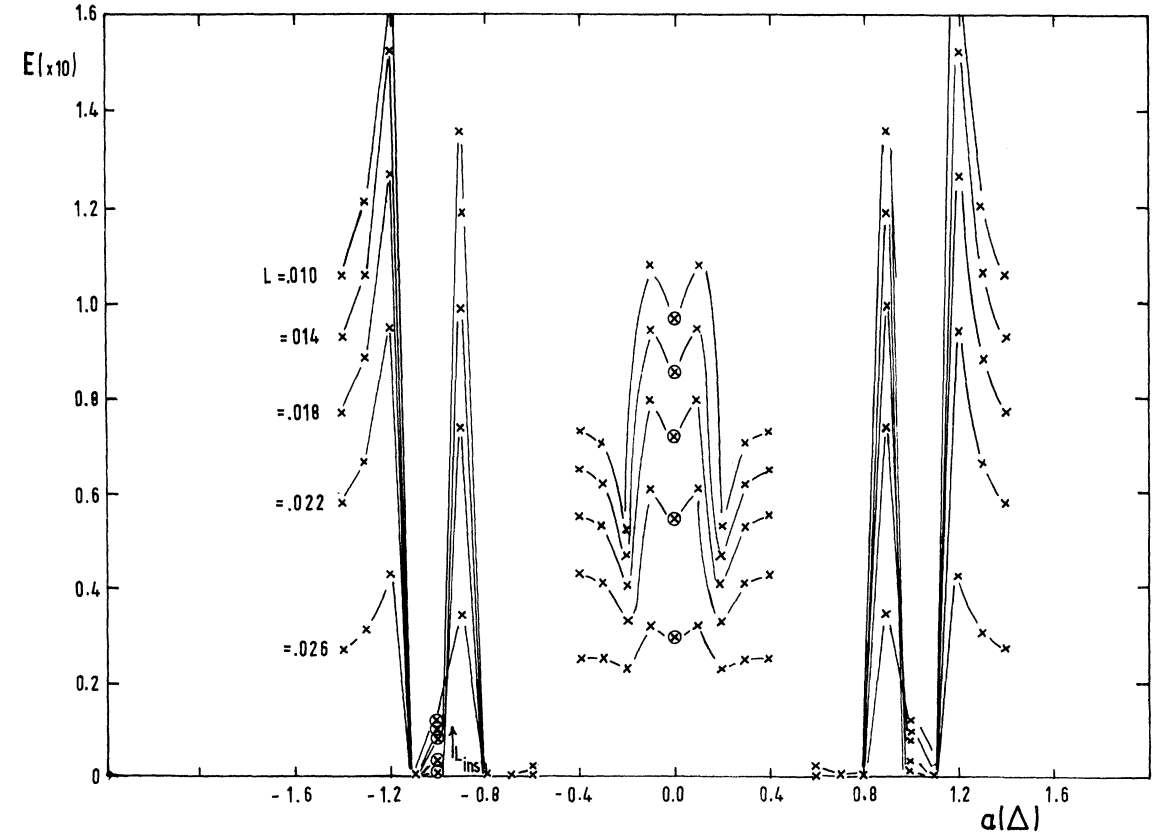

FIG. 2. Mode amplitudes as a function of cavity mode detuning for $L_0=0.3$, $ku=12\Delta$, $\gamma_{ab}=0.6\Delta$, and $\Delta=65$ MHz. N_2 in all cases is calculated for a tube of two-thirds the cavity length which is placed symmetrically in the cavity.

TABLE I. Solutions of the three-mode equations for $\Delta = 165$ MHz $\gamma_{ab} = 0.3\Delta$, $ku = 6\Delta$, $\gamma_a\gamma_b = 0.04\,\Delta^2$ and for a symmetrically placed active length equal to $\frac{2}{3}$ of the cavity length. In part D, entries are shown blank where ψ is nonconvergent.

A	E_1 (arb. units)					B	E_2 (arb. units)				
Loss	Detuning (units of Δ)					Loss	Detuning (units of Δ)				
	−0.4	−0.3	−0.2	−0.1	0.0		−0.4	−0.3	−0.2	−0.1	0.0
Solution with locking terms neglected						Solution with locking terms neglected					
0.028	0.0	0.0	0.0	0.0	0.0	0.028	0.57	0.21	0.18	0.16	0.19
0.026	0.0	0.04	0.0	0.0	0.21	0.026	0.40	0.30	0.30	0.29	0.30
0.024	0.37	0.37	0.35	0.30	0.35	0.024	0.0	0.37	0.38	0.38	0.38
0.022	0.53	0.52	0.50	0.48	0.44	0.022	0.0	0.43	0.45	0.45	0.44
0.020	0.65	0.64	0.61	0.61	0.52	0.020	0.0	0.49	0.51	0.51	0.49
0.018	0.75	0.73	0.71	0.72	0.59	0.018	0.0	0.53	0.56	0.56	0.55
0.016	0.84	0.82	0.79	0.81	0.66	0.016	0.0	0.58	0.61	0.61	0.59
0.014	0.92	0.90	0.87	0.89	0.71	0.014	0.0	0.62	0.65	0.65	0.63
0.012	0.99	0.97	0.94	0.97	0.76	0.012	0.0	0.65	0.69	0.70	0.67
0.010	1.06	1.04	1.01	1.04	0.81	0.010	0.0	0.69	0.73	0.74	0.71
Solution of full set of differential equations						Solution of full set of differential equations					
0.028	···	0.03	···	···	···	0.028	···	0.36	···	···	···
0.026	···	0.02[a]	···	···	0.21[a]	0.026	···	0.17[a]	···	···	0.21[a]
0.024	0.37	0.36[a]	0.33[a]	0.33	0.35[a]	0.024	0.0	0.38[a]	0.39[a]	0.36	0.35[a]
0.022	0.53	0.53[a]	0.51[a]	0.53	0.45[a]	0.022	0.0	0.50[a]	0.48[a]	0.34	0.45[a]
0.020	0.65	0.64	0.63	0.67	0.53	0.020	0.0	0.43	0.55	0.34	0.53
0.018	0.75	0.72	0.69	0.71	0.59[a]	0.018	0.0	0.51	0.56	0.44	0.59[a]
0.016	0.84	0.84	0.82	0.83	0.66[a]	0.016	0.0	0.63	0.61	0.41	0.65[a]
0.014	0.92	0.89	0.90	0.89	0.71[a]	0.014	0.0	0.67	0.63	0.49	0.71[a]
0.012	1.00	0.92	0.96	0.94	0.78[a]	0.012	0.0	0.70	0.65	0.48	0.78[a]
0.010	1.07	1.05	1.03	1.06	0.81[a]	0.010	0.0	0.64	0.78	0.50	0.81[a]

C	E_3 (arb. units)					D	ψ				
Loss	Detuning (units of Δ)					Loss	Detuning (units of Δ)				
	−0.4	−0.3	−0.2	−0.1	0.0		−0.4	−0.3	−0.2	−0.1	
Solution with locking terms neglected											
0.028	0	0.14	0.22	0.35	0	0.028					
0.026	0	0.28	0.31	0.37	0.21	0.026		41.5			0.0
0.024	0.54	0.38	0.38	0.39	0.35	0.024		2.2	2.00		0.0
0.022	0.76	0.45	0.44	0.42	0.45	0.022		3.15	3.47		0.0
0.020	0.93	0.51	0.49	0.44	0.52	0.020					
0.018	1.07	0.57	0.53	0.46	0.59	0.018					0.0
0.016	1.20	0.62	0.57	0.48	0.66	0.016					0.0
0.014	1.32	0.67	0.61	0.50	0.71	0.014					0.0
0.012	1.42	0.71	0.65	0.51	0.76	0.012					0.0
0.010	1.52	0.76	0.68	0.53	0.81	0.010					0.0
Solution of full set of differential equations											
0.028	···	0.28	···	···	···						
0.026	···	0.16[a]	···	···	0.21[a]						
0.024	0.53	0.38[a]	0.39[a]	0.36	0.35[a]						
0.022	0.63	0.37[a]	0.38[a]	0.34	0.45[a]						
0.020	0.71	0.56	0.42	0.34	0.53						
0.018	0.79	0.61	0.56	0.44	0.59[a]						
0.016	0.86	0.53	0.53	0.41	0.65[a]						
0.014	0.92	0.63	0.58	0.49	0.71[a]						
0.012	0.98	0.63	0.66	0.48	0.78[a]						
0.010	1.04	0.80	0.60	0.50	0.82[a]						

[a]Locking is predicted.

classed as unlocked situations.

Table I shows the steady-state values obtained from the unlocked equations together with the results from the integration of the full set of equations. It can be seen from the value of ψ whether or not locking is predicted (see Table I, part D). In cases where ψ remains an increasing function of time, Table I, parts A–C, shows that the final values of electric field amplitude are very close to those obtained directly from the reduced set of equations assuming no locking. In cases where locking takes place, the final electric-field values are, except at the line center where they are identical, no more than 15% different from the values given by unlocked approximation.

The matrix solution of the reduced set of equations for the unlocked case is simply the solution of the steady-state equations and as such is only valid if a three-mode unlocked steady state exists. If the modes are locked, or if the competition is sufficiently severe that one or more modes is extinguished, then these solutions are no longer valid. The solutions to the complete differential equations, however, do not suffer from this restriction. Table II shows the locked or unlocked state predicted by the full theory together with that predicted from the locking criterion discussed earlier when applied to the steady-state solution of the equations which excluded terms in ψ, for several inserted losses and detunings. Results are difficult to obtain very close to threshold because of the high numerical errors which appear in the calculations. Above threshold, however, a fairly well-defined pattern evolves. When the middle mode is at the line center, locking always occurs; for the other detunings, the modes are unlocked except for a region of locking for detunings in the region $-0.3\Delta \leq a \leq -0.2\Delta$ and inserted losses $0.024 \leq L \leq 0.020$. It can be seen that the locking criterion derived from the steady-state equations gives much the same results.

III. RESULTS

A. Mode Amplitudes

1. *Variation With Axial Mode Spacing* Δ

It is convenient to present the results in graphical form. In Figs. 2–4, the amplitudes of the three modes are plotted against detuning. It must be remembered that the actual oscillation frequencies of the modes are different from the passive cavity resonance frequencies because of the effects of mode pulling and pushing due to the nonlinear character of the gain medium.

Figures 2–4 show results for cavity lengths, corresponding to cavity mode spacings Δ, of 65, 130, and 400 MHz, respectively, and for the atomic parameters quoted in the appropriate figure captions. In Fig. 2, where the natural linewidth γ_{ab} is taken as 0.6Δ and the holes burned in the gain curve by the oscillating modes can be expected to overlap, it is clear that there is severe competition between the modes for the available gain. It can be seen that the outer modes with amplitudes E_1 and E_3 are competing for the same set of atoms and are constantly changing in relative magnitude as the detuning changes. This competitive behavior becomes increasingly marked as the cavity loss is decreased and at higher intensity the center mode is also severely affected by competition. For the larger cavity mode spacing as the results in Fig. 3 show, the situation is

TABLE II. Values of the locking criterion $A^2+B^2-\Sigma^2$ are given as + or −. Results of the integration of the full set of differential equations are given as U when the solutions are unstable in ψ, and S when they are stable in ψ. That is, there is consistency between the results of the full solution approach and that of the steady-state equations when $S+$ or $U-$ are listed. The regions of inconsistency are boxed. Columns A and C should be treated with caution since in C, E_1 tends to vanish and in A, E_2 tends to vanish, thus leaving only a two-mode situation to which the locking criterion does not apply.

	A. Δ=65 MHz					B. Δ=130 MHz					C. Δ=400 MHz				
Loss	Detuning					Detuning					Detuning				
	−0.4	−0.3	−0.2	−0.1	0.0	−0.4	−0.3	−0.2	−0.1	0.0	−0.4	−0.3	−0.2	−0.1	0.0
0.028	S−	S−	S−	S−	S−	−	−	−	−	−	U−	U−	U−	U−	U−
0.026	S−	S+	U−	U−	S+	U−	U−	U−	U−	S+	S−	S−	S−	S−	S−
0.024	U−	U−	U−	U+	S+	U−	S+	S+	U+	S+	S−	S−	S−	S−	S+
0.022	U+	U−	U−	U+	S+	U−	S−	S+	U+	S+	S−	S−	S−	S−	S+
0.020	U+	U+	U−	U+	S+	U−	S−	U−	U−	S+	S−	S−	S−	S−	S+
0.018	U+	U+	U−	U+	S+	U−	U−	U−	U−	S+	S−	S−	U−	U−	S+
0.016	U+	U+	U−	U+	S+	U−	U−	U−	U−	S+	U−	U−	U−	U−	S+
0.014	U+	U+	U−	U+	S+	U−	U−	U−	U−	S+	U−	U−	U−	U−	S+
0.012	U+	U+	U−	U+	S+	U−	U−	U−	U−	S+	U−	U−	U−	U−	S+
0.010	U+	U+	U−	U+	S+	U−	U−	U−	U−	S+	U−	U−	U−	U−	S+

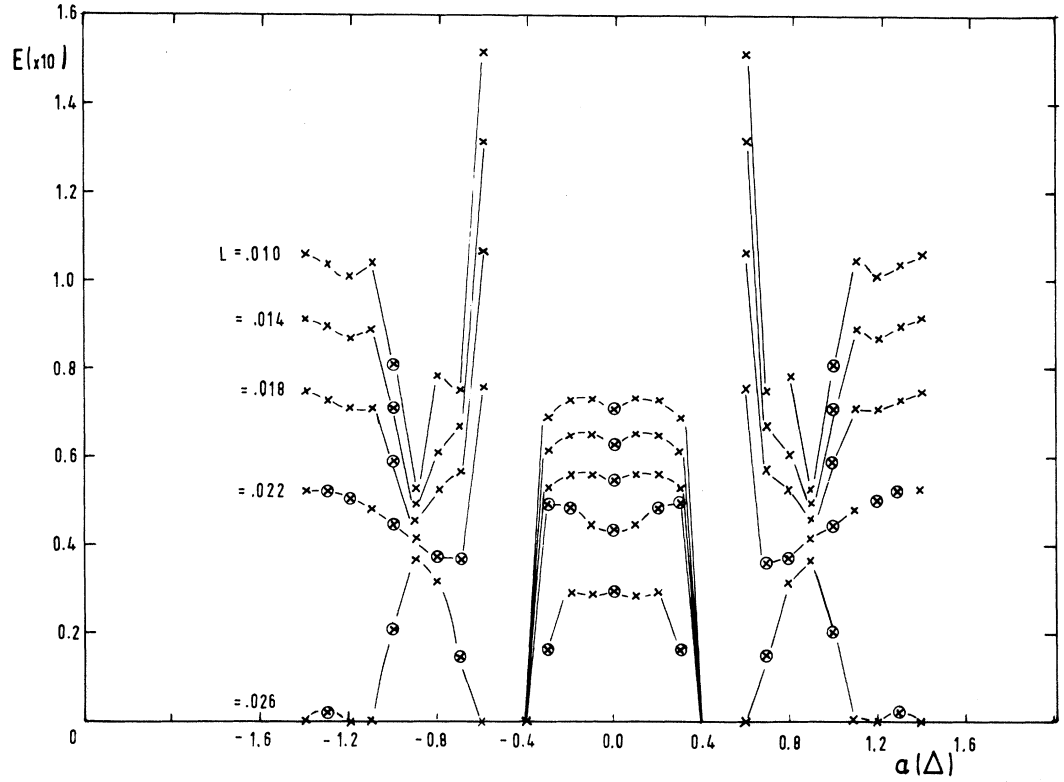

FIG. 3. Mode amplitudes as a function of cavity mode detuning for $L_0 = 0.03$, $ku = 6\Delta$, $\gamma_{ab} = 0.3\Delta$, and $\Delta = 130$ MHz.

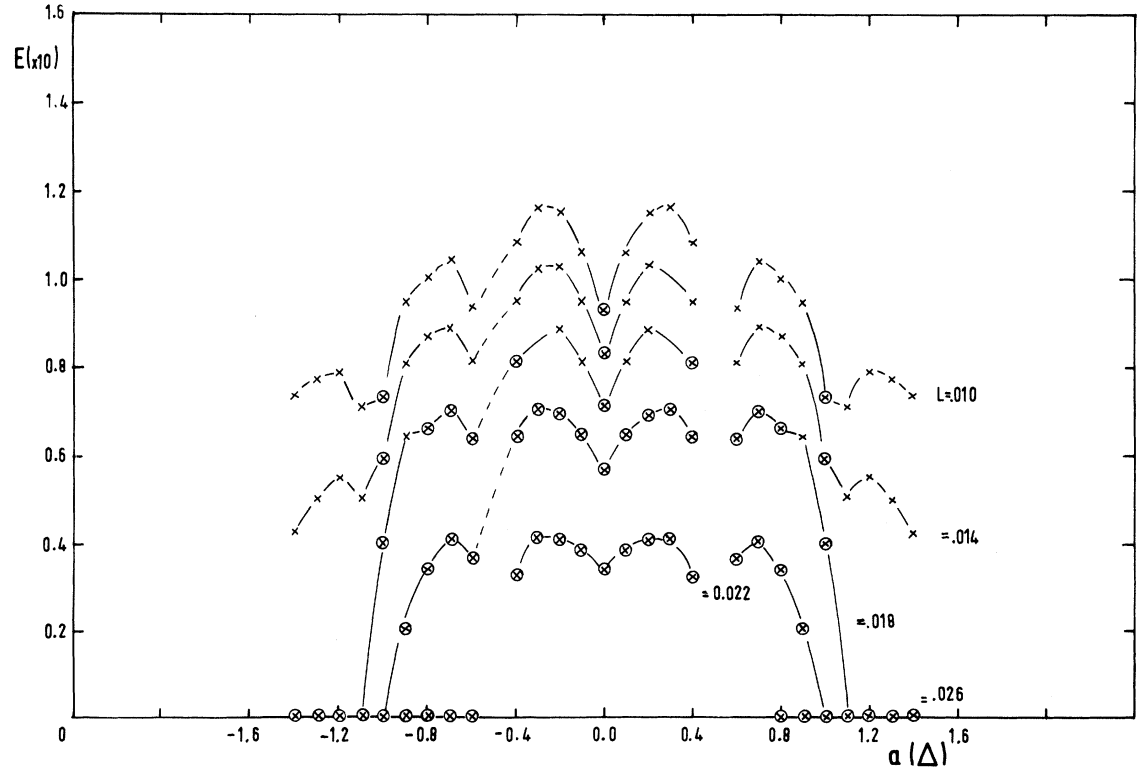

FIG. 4. Mode amplitudes as a function of cavity mode detuning for $L_0 = 0.03$, $ku = 2\Delta$, $\gamma_{ab} = 0.1\Delta$, and $\Delta = 400$ MHz.

a little different. The lower curves corresponding to near threshold behavior show much less severe competition than the corresponding curve in Fig. 2, but E_1 and E_2 are still destructively competing with each other.

The influence of the shape of the Doppler gain curve is shown, however, by the fact that it is the mode farther from the line center which loses intensity. For the higher intensity curve shown, this behavior is not apparent. It is interesting also to note that the center of the three modes E_2 exhibits a rise at the line center near threshold but a dip when the system is much above threshold. This is similar to the Lamb-dip behavior of a single-mode system. In Fig. 4 for a large axial-mode spacing, corresponding to $\Delta = 400$ MHz, the competition behavior is not severe enough to cause violent fluctuations in the intensity of E_1 and E_3 as the detuning changes, but their behavior is governed instead by the shape of the Doppler gain curve. It is, in fact, always the one further from the line center which loses. It is also clear in this case that the center mode has a higher intensity with respect to the outer ones, again because of the shape of the gain curve.

2. *Variation with Natural Linewidth* γ_{ab}

It would be expected that increasing the natural linewidth would increase mode competition. That this is indeed the case is seen by comparing Fig. 3 for $\gamma_{ab} = 0.3\Delta$ with Fig. 5 for $\gamma_{ab} = 0.4\Delta$. The general shape of the figures is much the same but the degree of competition is greater for the larger linewidth. The parameters of the 1.15-μ laser are used in the results shown in Figs. 6 and 7 and the same behavior is apparent.

B. Locking Behavior

Detailed information concerning the locking characteristics of the system for various combinations of the laser parameters can be found from the ψ tables (Tables III–IX). It will be seen in almost all cases for which a three-mode system is possible that when the cavity modes are symmetrically displaced about the line center, the system is locked. This is always $\psi = 0$-type locking. For parameters corresponding to the 0.633-μm He-Ne laser, there is another locking region for moderate intensities for detunings in the range $0.3 \geq a \geq 0.2$ for which $\psi \neq 0$. This region of lock-

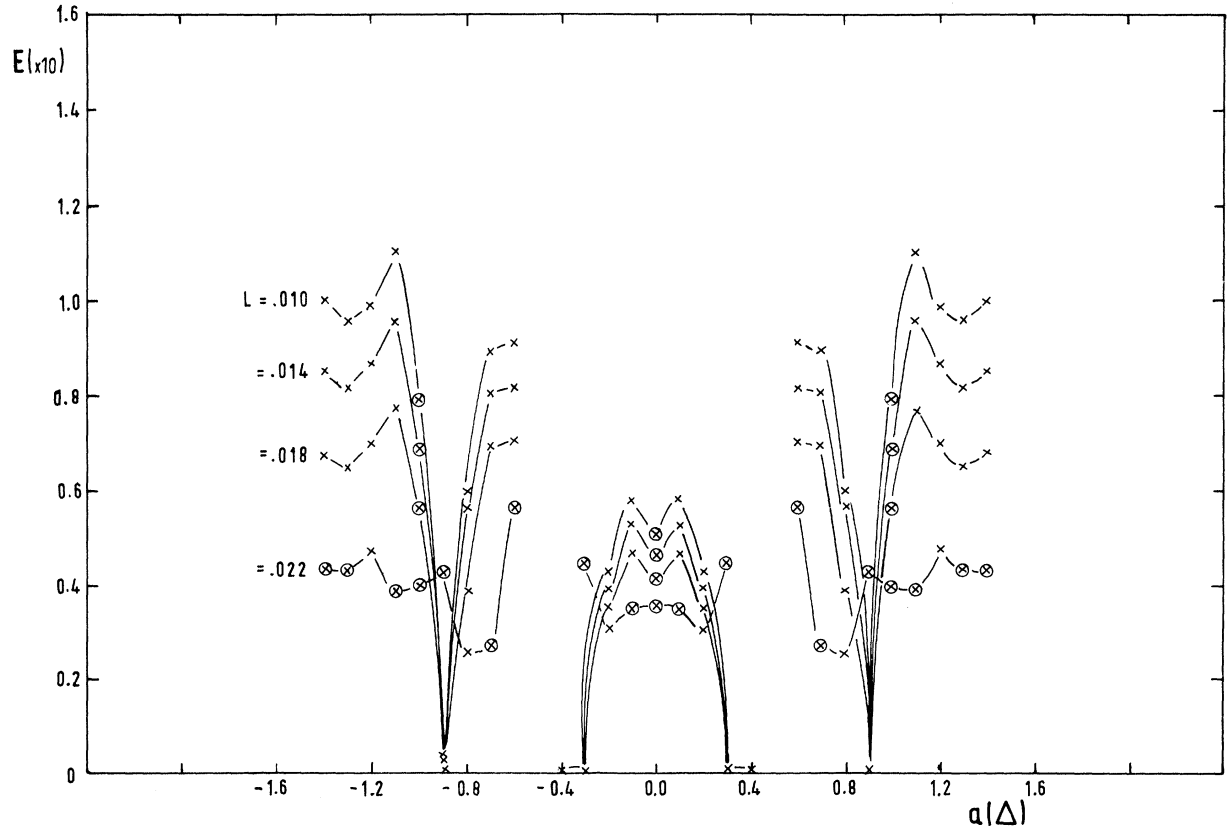

FIG. 5. Mode amplitudes as a function of cavity mode detuning for $L_0 = 0.03$, $ku = 6\Delta$, $\gamma_{ab} = 0.4\Delta$, and $\Delta = 130$ MHz.

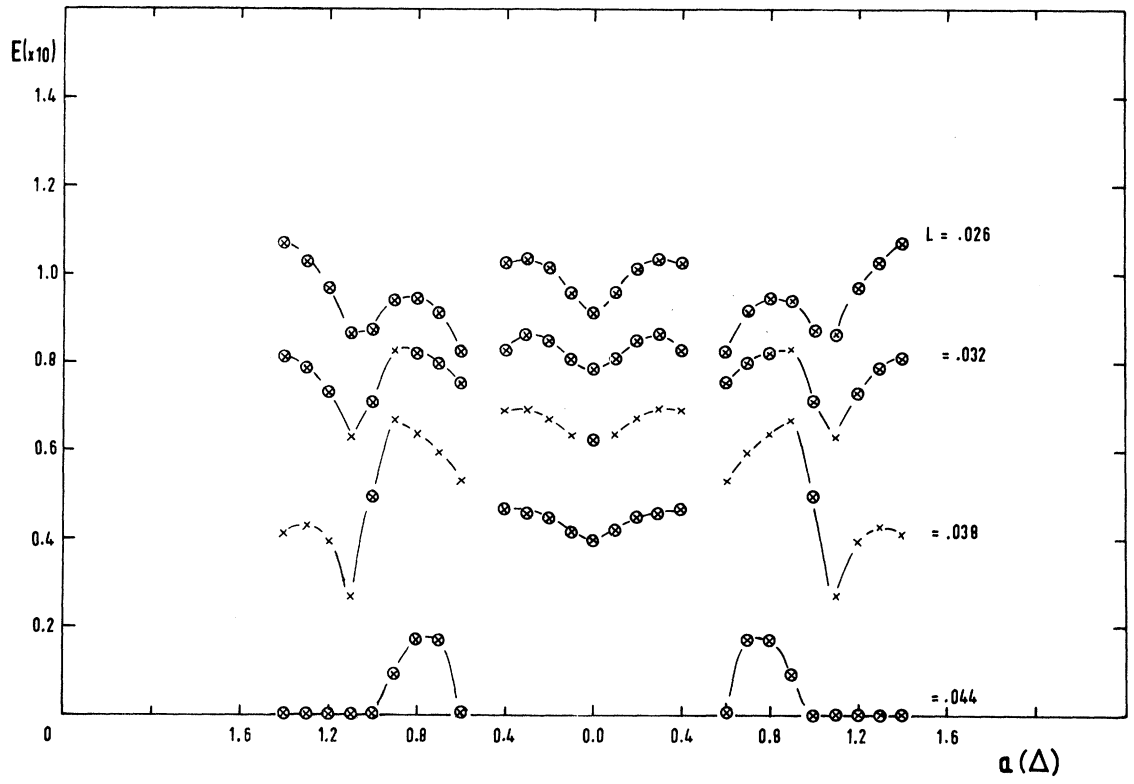

FIG. 6. Mode amplitudes as a function of cavity mode detuning for $L_0 = 0.05$, $ku = 4\Delta$, $\gamma_{ab} = 0.2\Delta$, and $\Delta = 130$ MHz.

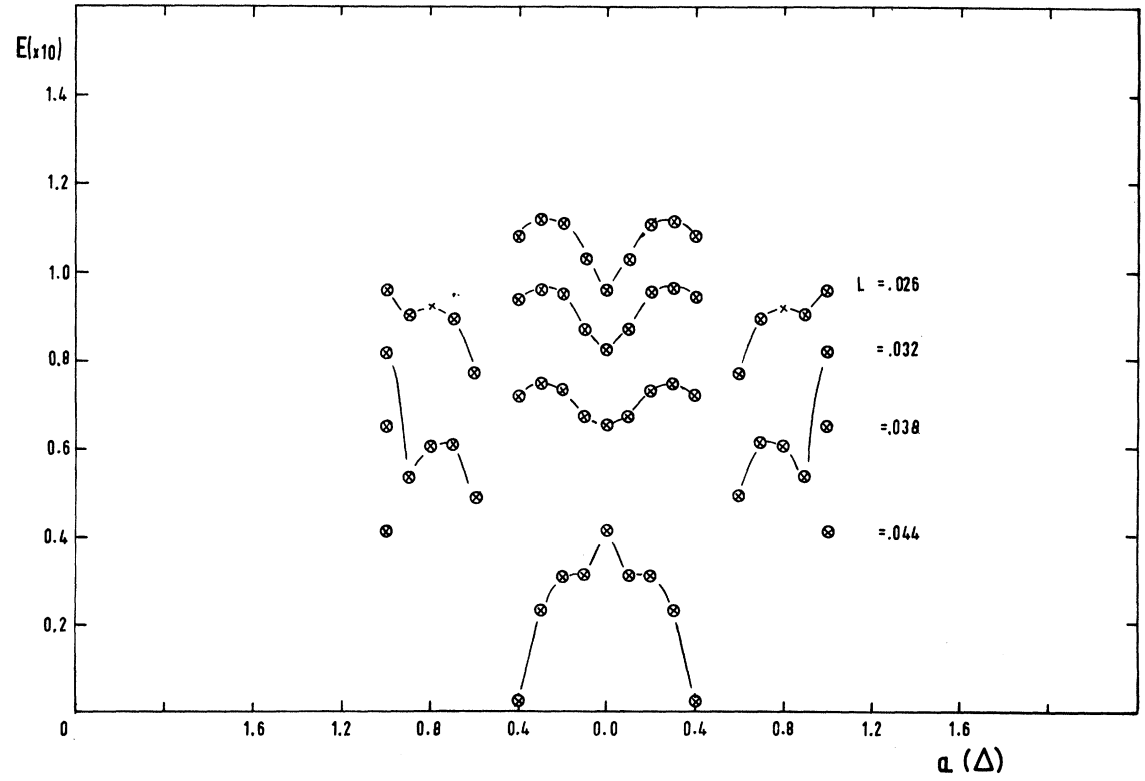

FIG. 7. Mode amplitudes as a function of cavity mode detuning for $L_0 = 0.05$, $ku = 2\Delta$, $\gamma_{ab} = 0.15\Delta$, and $\Delta = 260$ MHz.

TABLE III. Steady-state values of ψ for $L_0 = 0.03$, $ku = 12\Delta$, $\gamma_{ab} = 0.6\Delta$, and $\Delta = 65$ MHz. Unlocked steady states are shown blank.

Loss	Detuning (units of Δ)				
	−0.4	−0.3	−0.2	−0.1	0.0
0.028	0	0	0	5.10	0.0
0.026	9.67				0.0
0.024					0.0
0.022					0.0
0.020					0.0
0.018					0.0
0.016					0.0
0.014					0.0
0.012					0.0
0.010					0.0

TABLE IV. Steady-state values of ψ for $L_0 = 0.03$, $ku = 6\Delta$, $\gamma_{ab} = 0.3\Delta$, and $\Delta = 130$ MHz. Unlocked steady states are shown blank.

Loss	Detuning (units of Δ)				
	−0.4	−0.3	−0.2	−0.1	0.0
0.028					
0.026					0.0
0.024		2.35	2.14		0.0
0.022		3.13	3.36		0.0
0.020		9.88			0.0
0.018					0.0
0.016					0.0
0.014					0.0
0.012					0.0
0.010					0.0

TABLE V. Steady-state values of ψ for $L_0 = 0.03$, $ku = 2\Delta$, $\gamma_{ab} = 0.1\Delta$, and $\Delta = 400$ MHz. Unlocked steady states are shown blank.

Loss	Detuning (units of Δ)				
	−0.4	−0.3	−0.2	−0.1	0.0
0.028					
0.026	−0.4	−0.6	−0.9	−1.7	0.0
0.024	−0.6	−0.8	−1.2	−1.8	0.0
0.022	−0.7	−1.0	−1.4	−1.9	0.0
0.020	−0.9	−1.3	−1.7	−2.2	0.0
0.018	−1.3	−1.7	−0.9		0.0
0.016					0.0
0.014					0.0
0.012					0.0
0.010					0.0

TABLE VI. Steady-state values of ψ for $L_0 = 0.03$, $ku = 6\Delta$, $\gamma_{ab} = 0.4\Delta$ and $\Delta = 130$ MHz. Unlocked steady states are shown blank.

Loss	Detuning (units of Δ)				
	−0.4	−0.3	−0.2	−0.1	0.0
0.028	−19.4			−2.4	0.0
0.026	3.63	2.71		0.0	0.0
0.024	10.8				0.0
0.022					0.0
0.020					0.0
0.018					0.0
0.016					0.0
0.014					0.0
0.012					0.0
0.010					0.0

TABLE VII. Steady-state values of ψ for $L_0 = 0.05$, $ku = 4\Delta$, $\gamma_{ab} = 0.2\Delta$, and $\Delta = 130$ MHz. Unlocked steady states are shown blank.

Loss	Detuning (units of Δ)				
	−0.4	−0.3	−0.2	−0.1	0.0
0.053					
0.050	−1.4	−0.9	−0.6	−2.8	0.0
0.047	−0.5	−0.6	−0.8	−1.0	0.0
0.044	−1.1	−1.3	−1.6	−1.9	•••
0.041	−1.8	−8.3	−8.4	−2.3	0.0
0.038					0.0
0.035	−4.5				0.0
0.032	−2.5	2.5	−4.4		0.0
0.029	−2.8	3.0	2.6	−4.2	0.0
0.026	−3.0	3.4	3.0	2.6	0.0

TABLE VIII. Steady-state values of ψ for $L_0 = 0.05$, $ku = 2\Delta$, $\gamma_{ab} = 0.2\Delta$, and $\Delta = 65$ MHz. Unlocked steady states are shown blank.

Loss	Detuning (units of Δ)				
	−0.4	−0.3	−0.2	−0.1	0.0
0.041	−6.9	−6.9	−2.1	−1.5	0.0
0.038		−1.1	−1.4	−1.7	0.0
0.035	−1.1	−1.4	−1.6	−1.9	0.0
0.032	−1.3	−1.5	−1.8	−2.0	0.0
0.029	−1.5	−1.7	−1.9	−2.1	0.0
0.026	−1.6	−1.8	−2.0	−2.2	0.0
0.023	−1.9	−2.0	−2.2	−8.6	0.0
0.020				−8.7	
0.017					0.0
0.014					0.0

ing is sensitive to variation of the length and position of the laser tube in the cavity (N_2), and to the cavity length (Δ).

For small axial mode spacing, the delicate balance needed for locking appears to be upset by the severe mode competition (Table III). For large axial mode spacings (Table V), the influence of the shape of the Doppler gain curve is such that the outer mode either does not oscillate at all or only oscillates very weakly. Consequently, although there is a region from threshold up to medium values of the inserted loss where ψ is a constant, this is not really a three-mode system. When the inserted loss is reduced to allow stronger oscillation, the locking is no longer predicted mainly because of the increased effects of competition. Severe mode competition appears always to inhibit locking. When the linewidth γ_{ab} is large,

TABLE IX. Steady-state values of ψ for $L_0 = 0.05$, $ku = 2\Delta$, $\gamma_{ab} = 0.15\Delta$, and $\Delta = 65$ MHz.

Loss	Detuning (units of Δ)				
	−0.4	−0.3	−0.2	−0.1	0.0
0.053	−4.6	−3.6	−1.9	−0.96	0.0
0.050	−7.0	−3.6	−2.4	−1.2	0.0
0.047	−0.54	−0.64	−0.8	−1.9	0.0
0.044	−0.46	−0.62	−0.9	−1.3	0.0
0.041	−0.64	−0.87	−1.2	−1.6	0.0
0.038	−0.86	−1.1	−1.4	−1.8	0.0
0.035	−1.1	−1.3	−1.6	−2.0	0.0
0.032	−1.2	−1.5	−1.8	−2.1	0.0
0.029	−1.5	−1.7	−2.0	−2.2	0.0
0.026	−1.7	−8.2	···	−8.7	0.0

locking occurs only very near threshold or when the modes are in the symmetric position (Table VI).

The smaller Doppler width and larger maximum inserted loss of the 1.15 μm He-Ne laser produce a greater tendency towards locking, but the competition is more severe and the locking behavior is more erratic as a result (Tables VII–IX).

It is difficult to itemize in a general fashion under what conditions of $\Delta\nu_D$, Δ, γ_{ab}, and inserted loss, locking is to be expected. Examination of Tables III–IX shows the results for a variety of values for these parameters.

C. Beat Frequencies

Figures 8–11 show computed results for the difference frequencies of the polarization components $(\nu_j - \dot{\phi}_j) - (\nu_i - \dot{\phi}_i)$ from Eqs. (2). Two general points should be made concerning the application of these results to a real experimental situation. Firstly, it is not possible to distinguish experimentally between the frequency ν_i and the rate of change of phase angle $\dot{\phi}_i$, and it is convenient, therefore, to calculate the experimentally measurable beat frequency $(\nu_j - \dot{\phi}_j) - (\nu_i - \dot{\phi}_i)$. Secondly, the present section calculates the frequency of the polarization components, but these results should be used in conjunction with the earlier results for mode amplitudes in order to determine whether an experimentally measurable beat component actually exists.

In Figs. 8–10, the beat frequency $\nu_2 - \nu_1$ is plotted (where ν_1 is written instead of $\nu_1 - \dot{\phi}_1$) for three values of Δ as a function of the detuning a of the middle cavity mode from the line center. In order to simplify the diagrams, $\nu_3 - \nu_2$ is not shown but can easily be found by reflecting the curves for $\nu_2 - \nu_1$ about the line center ($a = 0$). In each figure the results are plotted for six values of cavity loss. The laser parameters are the same as those employed in the calculation of the mode amplitude results displayed in Figs. 2–4, respectively. All points where locking occurs are ringed on the figures.

The functional dependence of the oscillation frequencies on the mode amplitudes is described by Eq. (2). In order to interpret the meaning of these equations, it is often helpful to bear in mind some of the more phenomenological ideas due to Bennett.[3] Three processes may be recognized in Eq. (2). Consider the equation for ν_1. The basic frequency is the cavity resonance frequency Ω_1. The nonlinear character of the gain medium gives rise to a "pulling" term σ_1, but the oscillating mode itself distorts the shape of the gain curve and produces the so-called frequency "pushing" effect due to "hole burning." This is described by the term $\rho_1 E_1^2$. The three terms Ω_1, σ_1, and $\rho_1 E_1^2$ are solely functions of the medium and the intensity of the mode under consideration. Hole-burning effects caused by the other two oscillating modes are included in the terms $\tau_{12}E_2^2$ and $\tau_{13}E_3^2$. The remaining terms are phase-dependent interaction terms.

The mode frequencies are seen, therefore, to be very strongly dependent on the mode amplitudes. It might be expected, therefore, that the beat frequency results would display similar behavior with regard to intensity and axial mode spacing as the amplitude results. This is indeed the case. Figure 8 shows the computed values of the beat frequency $\nu_2 - \nu_1$ for a small axial mode spacing $\Delta = 65$ MHz. As expected, the variation of beat frequency with detuning becomes much more violent as the laser intensity is increased. This is a direct result of the increasing competition between the oscillating modes.

A more common situation is shown in Fig. 9 for a cavity mode spacing of $\Delta = 130$ MHz. It can be seen that the picture here is much more stable, the beat frequency versus detuning curves being very smooth except for $a = 0.4$, where it can be seen from the amplitude curves that the central mode is highly attenuated.

Figure 10 shows the results for a large cavity mode spacing of $\Delta = 400$ MHz. For losses of $L = 0.006$ up to $L = 0.014$, the curves exhibit the unlocked pattern with quite a large frequency difference between the $\nu_3 - \nu_2$ beat and the $\nu_2 - \nu_1$ beat. It will be realized that in these figures this frequency difference is obtained from the frequency difference between points for the same $|a|$ but on opposite sides of the line center. For high losses, $L \geq 0.022$, the shapes of the curves (Fig. 9) are symmetric about the line center as is typical for the case of mode locking. This is not particularly useful, however, as the amplitude curves show that in this case there are only two modes os-

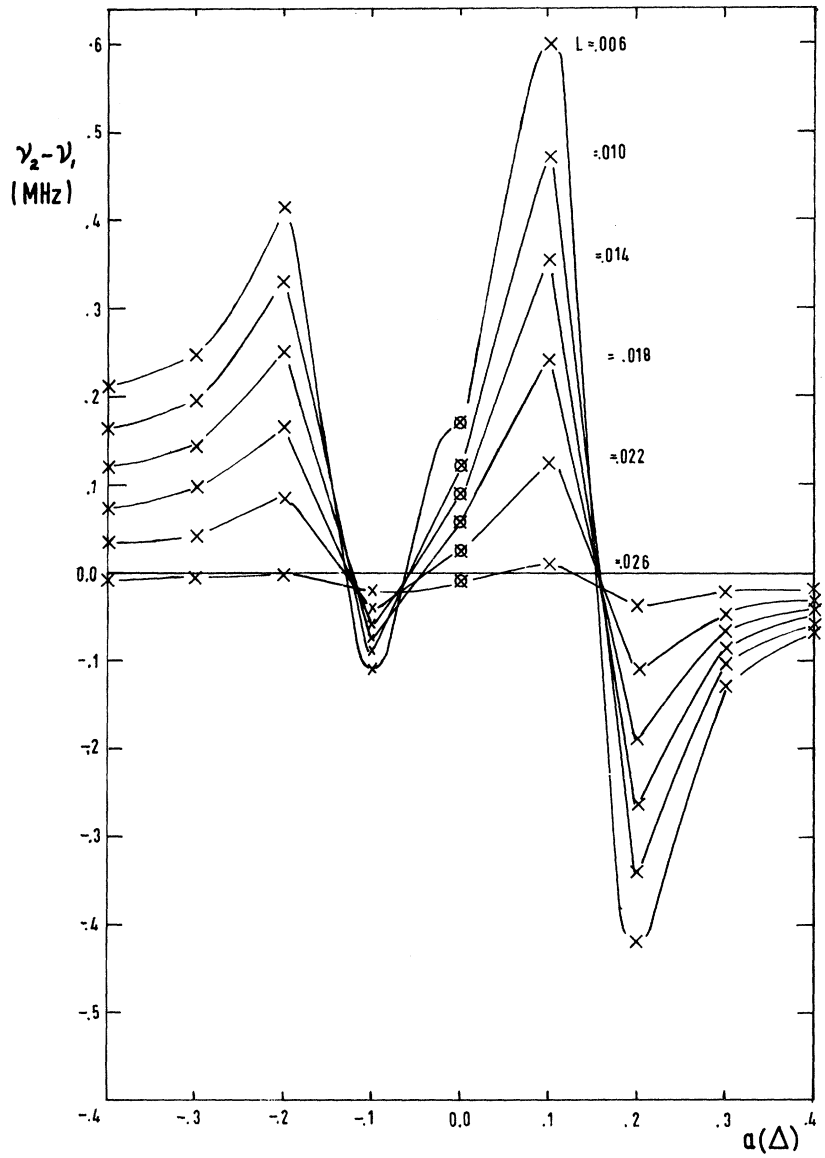

FIG. 8. Beat frequency $\nu_2-\nu_1$ as a function of cavity mode detuning for $L_0=0.03$, $ku=12\Delta$, $\gamma_{ab}=0.6\Delta$, and $\Delta=65$ MHz.

cillating. There will, therefore, be only one detectable beat frequency. For intermediate losses, $L\sim 0.018$, very interesting behavior occurs (Fig. 10). As the cavity modes are detuned to lower frequency, the frequency of the $\nu_2-\nu_1$ beat preserves its unlocked value until $a\sim 0.3$ when locking occurs and the frequency jumps to a value the same as that of the $\nu_3-\nu_2$ beat. This value is very close to the frequency that would be expected for $\nu_3-\nu_2$ in an unlocked state. This is precisely the kind of behavior reported in experimental observations by Jones *et al.*[13] The experimental conditions employed corresponded to the case of the medium value for Δ and, as has been seen, this gives a region where mode competition is not so fierce as to remove the possibility of locking and where a three-mode solution is a real possibility. Had Δ been appreciably smaller or appreciably larger, agreement would not have been so obvious.

For the case of the medium Δ the results of Fig. 9 have been redrawn to plot frequency versus loss for the detuning $a=0.3$ (Fig. 11). This may be compared with experimental results given by Jones *et al*, for the coincidence of the $\nu_2-\nu_1$ and $\nu_3-\nu_2$ beat frequencies, as locking occurs.

D. Time Development

As has been mentioned earlier in Sec. II, which was concerned with the evaluation of the final steady-state amplitudes and frequencies, the integration of the equations was started from initial conditions near

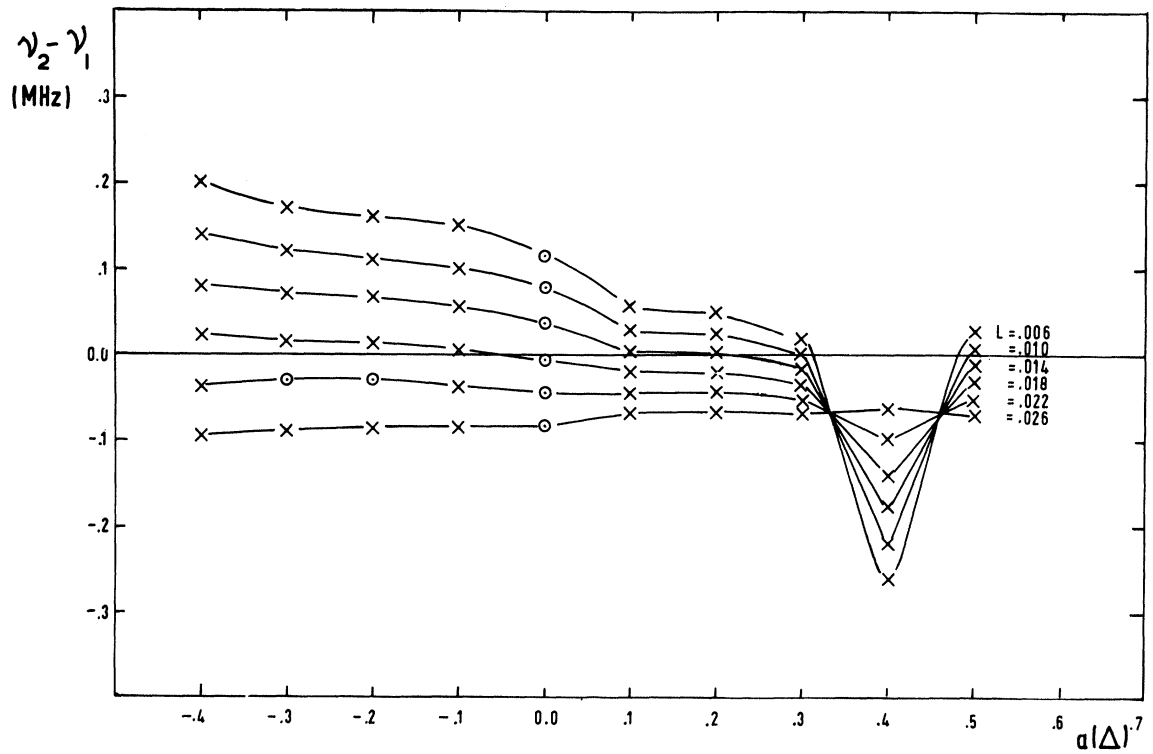

FIG. 9. Beat frequency $\nu_2-\nu_1$ as a function of cavity mode detuning for $L_0=0.03$, $ku=6\Delta$, $\gamma_{ab}=0.3\Delta$, and $\Delta=130$ MHz.

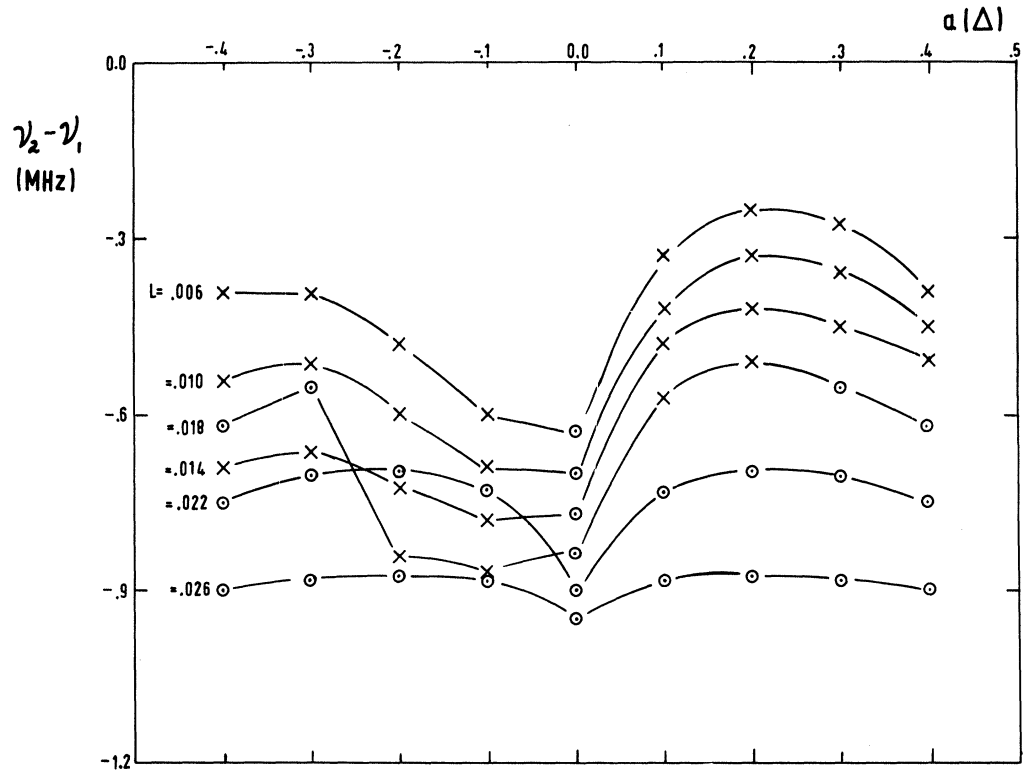

FIG. 10. Beat frequency $\nu_2-\nu_1$ as a function of cavity mode detuning for $L_0=0.03$, $ku=2\Delta$, $\gamma_{ab}=0.1\Delta$, and $\Delta=400$ MHz.

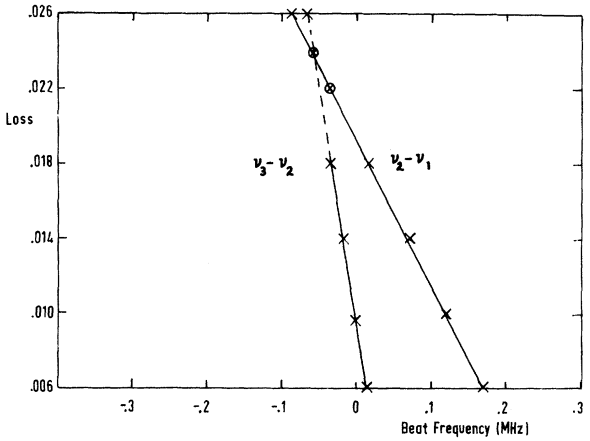

FIG. 11. Beat frequencies $\nu_2-\nu_1$ and $\nu_3-\nu_2$ as a function of inserted loss for a detuning of $a=0.3$, $L_0=0.03$, $ku=6\Delta$, $\gamma_{ab}=0.3\Delta$.

to the steady-state values in order to save computing time. If very small amplitudes are chosen for the initial conditions the integration can be used to predict the time development of the solutions for mode amplitudes. The particular solutions shown in Fig. 12 are for parameters corresponding to the 1.15-μ laser. This was chosen as an example since the smaller Doppler width makes the behavior with respect to detuning and inserted loss more explicit. Solutions are shown for four values of loss and for a detuning of $a=-0.4$ which is a position where the three modes have very different amplitudes. The initial amplitudes in these calculations were chosen to be $\sim 10^{-8}$ of the steady-state amplitudes.

Some general results may be noted. The rise time is dependent on the final steady-state amplitude – the higher the final amplitude, the faster the initial rise. E_2 is the amplitude of the mode nearest to the center of the gain curve and therefore the strongest of the three in this situation. It has an initial peak which falls very gradually to the final steady value. This fall is accompanied by a rather slow rise of E_1 and E_3.

In considering rise times as a function of amplitude, it is only found possible to compare the evolution of E_i for one set of laser parameters with E_i for another. It is not easy to compare, for example, the behavior of E_1 for one value

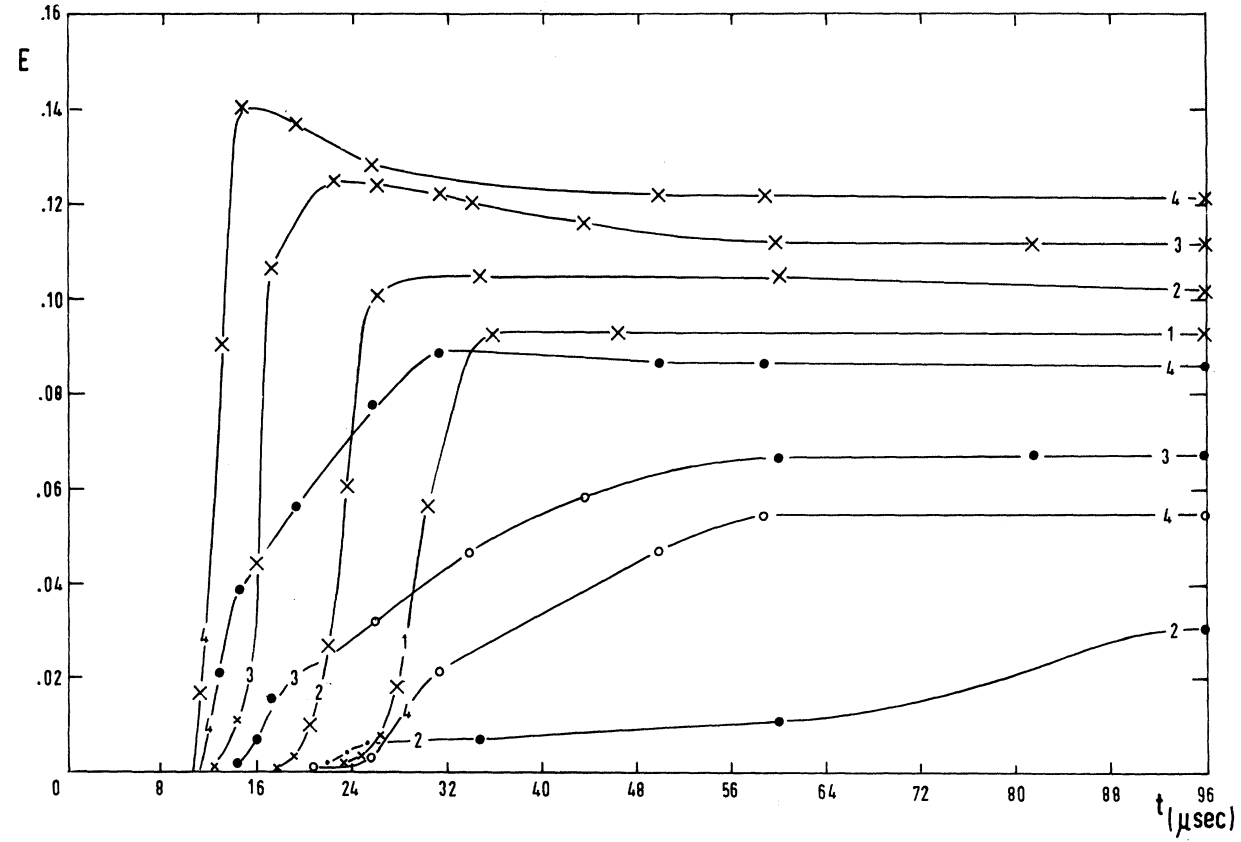

FIG. 12. Time development of the mode amplitudes for various conditions and for laser parameters $ku=4\Delta$, $\gamma_{ab}=0.2\Delta$, $\Delta=130$ MHz, and detuning $a=0.4\Delta$. Curves (1) correspond to a loss of $L=0.032$; curves (2) correspond to a loss of $L=0.029$; curves (3) correspond to a loss of $L=0.023$; curves (4) correspond to a loss of $L=0.017$.

of loss with E_2 for another. This is because the rates of rise of the three modes are not independent but are strongly linked via their mutual interactions.

The most significant feature of the results shown in Fig. 12 is the delay time ~10 μsec between the start of the oscillation and the point at which the mode amplitude is 5% of its peak value. The rise time from 5 to 95% of peak amplitude for E_2 for a small loss ($L = 0.017$) is 2.4 μsec and for the largest loss tried is 9.6 μsec ($L = 0.032$). The rise time of E_2 is shorter than that of E_1 for all losses shown. It will be noticed from Fig. 12 that the third mode is only present for the chosen laser parameters when $L = 0.017$ and then the rise time of E_1 is shorter than that of E_3. It is clear that, for a given value of loss, the more intense the mode the quicker its rise time and the shorter the delay time. For the detuning considered, E_2 is greatest for the lowest inserted loss. Its associated delay time is less than for E_2 corresponding to larger inserted losses. Also the delay times of E_1 and E_3 are less than their counterparts associated with higher losses. Thus the rise times and delays are clearly to be associated with the relative gain of the laser. The whole problem of time development is discussed elsewhere.[22] The time scales are in agreement with what might be expected.[23]

IV. CONCLUSIONS

The unabbreviated Lamb equations for the amplitude and frequency of three modes have been numerically integrated, and detailed information about the way in which the modes interact has been obtained. Considerable insight has been gained about the beat frequencies between the modes in terms of the mode intensities; and the conditions for self-locking to occur have been interpreted in terms of mode competition and the ratio of mode separation to the Doppler width of the gain profile. The time development of the equations allows the dynamic growth of the amplitudes to be studied and the effect of competition between the modes is manifested by the way in which the three modes attain their steady-state amplitudes.

The numerical integration of the complete set of equations, which include the phase-dependent terms, gives a much more complete picture of the three-mode process than any other approach used to date. Comparisons have been made here with other published work where approximations have been made, and the quality of the approximations has been evaluated.

Although the calculations have been applied to real systems, operating with reliable gains and mode separations, the calculations are somewhat idealized. For example, the values of γ_a, γ_b, and γ_{ab} are the pressure-independent values and the Doppler-broadened gain curve is taken to be symmetric, thus corresponding to a He-Ne laser with a single Ne isotope. However, the essential nature of the three-mode behavior will not be altered by the pressure broadened values of the γ's and the calculation could be reproduced in its entirety for the appropriate corrected value of γ if very specific information were required.

The general problem of the time evolution of the mode amplitudes is being tackled at the moment. In particular, it will be interesting to correlate the delay and risetime of the modes with the steady-state amplitudes in a general way, and to study the impact of locking on the same parameters. The quality of the solutions given in this paper would be best tested, and by implication the full Lamb theory would be well tested, if experimental data were available on the individual mode intensities, frequencies, risetimes, and locking characteristics of a three-mode laser as a function of loss and detuning.

ACKNOWLEDGMENTS

We wish to thank Dr. R. F. Carswell for many helpful discussions concerning the numerical analysis involved in this work, and Mrs. M.R. Beattie for many useful suggestions concerning the computer programs that were developed.

---

*Present address: Programming Branch, Computer Systems, Engineering Division, International Computers Ltd., Stevenage, Herts, England.

[1]W. E. Lamb, Jr., Phys. Rev. 134, 1429 (1964).

[2]A. Schawlow and C. H. Townes, Phys. Rev. 112, 1940 (1958).

[3]W. R. Bennett, Jr., Phys. Rev. 126, 580 (1962).

[4]A. Javan, W. R. Bennett, Jr., and D. R. Herriott, Phys. Rev. Letters 6, 106 (1961).

[5]A. G. Fox and T. Li, Bell. Syst. Tech. J. XL, 453 (1961).

[6]R. L. Fork and M. A. Pollack, Phys. Rev. 139, A1408 (1965).

[7]R. A. McFarlane, Phys. Rev. 3, A543 (1964).

[8]L. Allen, D. G. C. Jones, and M. D. Sayers, J. Phys. A 2, 87 (1969).

[9]M. H. Crowell, IEEE J. Quant. Electron. QE-1, 12 (1965).

[10]O. L. Gaddy and E. M. Schaefer, Appl. Phys. Letters 19, 281 (1966).

[11]T. Uchida, IEEE J. Quant. Electron. QE-3, 7 (1967).

[12]T. Uchida and A. Ueki, IEEE J. Quant. Electron.

QE-3, 17 (1967).
[13]D. G. C. Jones, M. D. Sayers, and L. Allen, J. Phys. A 2, 95 (1969).
[14]L. Allen and D. G. C. Jones (unpublished).
[15]D. O. Riska and S. Stenholm, Phys. Letters 30A, 16 (1969).
[16]M. Sargeant, III (private communication).
[17]L. Allen, D. G. C. Jones, and M. D. Sayers, J. Sci. Instr. 1, 133 (1968).
[18]J. A. Dobrowolski, J. Sci. Instr. 2, 429 (1969).
[19]L. Fox, *Numerical Solution of Ordinary and Partial Differential Equations* (Pergamon, Oxford, 1962).
[20]S. E. Harris and O. P. McDuff, IEEE J. Quant. Electron. QE-1, 245 (1965).
[21]O. P. McDuff and S. E. Harris, IEEE J. Quant. Electron. QE-3, 101 (1967).
[22]L. Allen and M. D. Sayers (unpublished).
[23]G. K. Born, IEEE J. Quant. Electron. QE-5, 67 (1969).

PHYSICAL REVIEW A VOLUME 1, NUMBER 6 JUNE 1970

Stimulated Modulational Instabilities of Plasma Waves

Akira Hasegawa
Bell Telephone Laboratories, Murray Hill, New Jersey 07974
(Received 23 June 1969; revised manuscript received 8 December 1969)

Nonlinear coupling of a modulated wave and a low-frequency mode is shown to produce a resonant interaction and instability when the Cherenkov condition $v_p = v_g \cos\theta$ is satisfied for the phase velocity v_p of the low-frequency mode, the group velocity v_g of the modulated wave, and the angle θ between the two wave vectors. This effect stimulates the self-trapping (modulational instability) or self-focusing of the modulated wave. Examples are shown for the cases of couplings between plasma cyclotron waves and magnetohydrodynamic (MHD) modes.

I. INTRODUCTION

Recently, the propagation of modulated waves in a nonlinear dispersive medium has aroused considerable interest in the self-focusing[1] or self-trapping[2] of laser beams and in the modulational instability of a nonlinear plasma wave.[3,4] Such an effect has been represented[5] by a Schrödinger equation for the amplitude of the modulated wave φ with a nonlinear potential term that is proportional to $|\varphi|^2$, i.e.,

$$i\frac{\partial\varphi}{\partial t} - \frac{\partial\omega}{\partial|\varphi|^2}(|\varphi|^2 - |\varphi_0|^2)\varphi + \frac{1}{2}\frac{\partial v_g}{\partial k}\frac{\partial^2\varphi}{\partial x^2} = 0. \quad (1)$$

The modulation has been shown to become unstable when the potential is attractive[1]; i.e., when

$$\frac{\partial\omega}{\partial|\varphi|^2}\frac{\partial v_g}{\partial k} < 0.$$

In the present paper, we present a new process that leads to a similar instability. In this case, the instability is due to a coupling of the modulated wave with a low-frequency nondispersive mode that may coexist in the same medium.

In this Introduction, we describe the general idea of the process. Consider a wave with slowly varying amplitude $\epsilon\varphi(x,t)\,e^{i(kx-\omega t)}$, where ϵ is a small parameter. A second-order nonlinearity will generate a perturbation of the form $\epsilon^2|\varphi(x,t)|^2$ and $\epsilon^2\varphi^2(x,t)\,e^{2i(kx-\omega t)}$. If the medium can propagate a low-frequency and long-wavelength mode, the slow perturbation, $\epsilon^2|\varphi(x,t)|^2$, will then excite this mode. We represent this mode by $\epsilon^2 V(x,t)$. If the medium is nondispersive at low frequencies, the equation describing V to lowest order may be written as an inhomogeneous linear equation with a source term proportional to $|\varphi|^2$, i.e.,

$$DV(x,t) = \alpha|\varphi(x,t)|^2. \quad (2)$$

In Eq. (2), α is the coupling coefficient, and D is a linear differential operator involving $\partial/\partial t$ and $\partial/\partial x$, having the form

$$D = \prod_{j=1}^{n} d_j\left(\frac{\partial^2}{\partial t^2} - v_{pj}^2\frac{\partial^2}{\partial x^2}\right), \quad (3)$$

where d_j is a constant, and the v_{pj} are the characteristic phase velocities ($j = 1, 2\cdots n$) of the low-frequency modes. Because a linear wave packet propagates at the group velocity v_g, the space and time dependency of φ in the right-hand side of Eq. (2), should be of the form $(x - v_g t) \equiv \xi$ in the lowest order. Equation (1) then assumes the form

$$\prod_{j=1}^{n} d_j\left(v_g^2 - v_{pj}^2\right)\frac{\partial^{2n}V}{\partial\xi^{2n}} = \alpha|\varphi|^2. \quad (4)$$

On the other hand, if the medium is linear but dispersive for the modulated high-frequency mode